Radiation Pattern, Surface Current Distribution, and Q-Factor Improvement Technique Using DMS CSPA: Part-II

Elliot O. Omoru and Viranjay M. Srivastava
Department of Electronic Engineering, Howard College,
University of Kwazulu-Natal, Durban-4041, South Africa
Email: {omoruelliot, viranjay}@ieee.org

***Abstract*—**In order to improve the efficiency, reliability, and accuracy during fabrication of antenna in 5G regime of frequencies, a Double-Material Substrate (DMS) Cylindrical Surrounding micro-strip fed Patch Antenna (CSPA) has been designed for use in 2.4/5.8 GHz WLAN, 2.5/5.15 GHz WiMAX wireless standards, 5.9 GHz Intelligent Transportation Society (ITS) band (5.85-5.925 GHz) and middle band of 5G technology (2.3 GHz ~ 2.4 GHz and 2.5 GHz ~ 2.69 GHz). The proposed antenna addresses the negative effect of dimension inaccuracy caused by the high permittivity substrate material used in CSPA. The antenna was designed, simulated, and thoroughly analyzed on the basis of the radiation pattern, surface current distribution, and Q factor. Findings reveal that the DMS CSPA showed a worthy radiation pattern and Q-factor of 3.62 and 2.31 at 2.68 GHz and 5.55 GHz bands, respectively. The radiation plots of simulation results present the angular width values between 45^0 ~ 104^0, showing a wider coverage area with minimal sidelobe level between -4.4 dB ~ 11.9 dB for the E-planes and H-planes at both resonance frequencies.

***Index Terms*—**Bandwidth, Cylindrical Surrounding Patch Antenna (CSPA), radio-frequency, S-parameter, WiMAX, WLAN

I. Introduction

The microstrip antennas are useful in 5G/WLAN/WiMAX applications at multiple frequency bands employing IEEE 802.11, 802.16, and 5G standards [1]-[3]. These standards have resulted in improved Quality of Standard (QoS), especially with the introduction of the WiMax (802.16) protocol. The standard WLAN/WiMAX frequency bands can be categorized into three large bands: *2.4* GHz -*2.7* GHz, *3.3* GHz - *3.7* GHz, and *5.15* GHz - *5.85* GHz. The *802.16* m standard is a more modern WiMAX standard. In the 5G regime, three operational bands have been chosen [4]-[6]. The *802.16* m standard is extremely effective (low bands fall under the *1* GHz band, medium bands between the *1* GHz and *6* GHz bands, and millimeter-wave bands as frequencies above *24* GHz). Now, with the introduction of 5G technology into the telecommunication industry, companies are integrating the 802.11 and 802.16 technology with the 5G technology because most countries have chosen their medium band of 5G technology as bands that fall within the lower bands of WiLAN/WiMAX standard (*2.4* GHz ~ *2.69* GHz). The 5G medium bands fall within the WiMAX standard of 802.16 m which is designed to operate from frequencies ranging from *2.3* GHz ~*2.4* GHz and *2.5* GHz ~ *2.69* GHz [7]-[9]. Incorporating all three technologies into a single antenna device will allow greater data speeds over large distances and provide a wide bandwidth with little interference. This will be especially beneficial as the transition from 4G to 5G technology progresses.

Furthermore, one form of microstrip antenna that will be very useful in the technology integration process at 5G regime of frequencies is the cylindrical conformal. This type of antenna has been observed to have a wider coverage area as presented in ref. [10]–[13]. The cylindrical surrounding patch antenna (which is a 360^0 rotated cylindrical variant of the rectangular planar patch antenna) is created using a transformation approach in which the width of the planar patch forms an arc in the cylindrical structure's H-plane [14]-[16].

For efficiency enhancement and technology integration, a wide-band horizontally polarized omni-directional antenna with a cylindrical ring dielectric was proposed by *Liu et. al.* [17] over the frequency range of *1.63* GHz to *2.8* GHz. The observed reflection coefficient was less than *10* dB, covering *52.8* % of the 2G/3G/LTE spectrum. Also, to achieve a low profile and broadside radiation, *Scardelletti et. al.* [18] have presented a cylindrical slot and folded slot antennas on Teflon and Alumina. Using a *1.27* cm diameter Teflon substrate, at *7* GHz, a gain of *1.5* dB (slot) and *2.8* dB (folded slot) was realized.

In this present research work, radiation pattern, surface current distribution, and Q-factor have been presented for designed DMS CSPA. This work is in continuation of the author's published work in ref. [19]. The proposed antenna has been designed for *2.4/5.8 GHz* WLAN, *2.5/5.15* GHz WiMAX wireless standards, *5.9 GHz* ITS band (*5.85* GHz - *5.92* GHz) allocated for use related to Dedicated Short-Range Communications (DSRC) for vehicle-to-vehicle communication, and middle band of 5G technology used in the United States and Canada (*2.3* GHz ~ *2.4* GHz and *2.5* GHz ~ *2.69* GHz) [20]-[22]. The proposed antenna is

Manuscript received September 2, 2021; revised April 15, 2022.
Corresponding author email: omoruelliot@ieee.org).
doi:10.12720/icm.17.5.393-398

a solution to the degraded performance of antenna design at high frequency using high dielectric permittivity materials. The methodology adopted could be used as a technique for improving VSWR and bandwidth. This paper has been organized as follows: Section II gives an analytical overview of the proposed DMS CPA. Section III analysis the proposed antenna based on radiation pattern, surface current, and Q-factor at various frequency bands. Finally, Section IV concludes the work and recommends the future aspect.

II. Analytical Overview of Proposed Dual-Band Double-Material Substrate CSPA

The decreased size of an antenna fabricated at high frequency employing high dielectric permittivity materials causes the poor performance of the microstrip patch antenna [23], [24]. When the size of the antenna becomes too small, the radiation efficiency is affected (e.g., using substrate materials with high dielectric constants increases impedance mismatch, thus degrading the radiation efficiency). A substrate material with a low dielectric permittivity is employed to address this issue, resulting in a bigger antenna size with higher radiation efficiency. The resultant antenna, however, may be too big to fit within the mobile device. *Omoru and Srivastava* [25] have designed CSPA with a double-material demonstrated for 5G/WLAN/WiMAX application in a 5G regime to solve device fitting and dimension inaccuracies during the fabrication process.

This proposed antenna has been designed using polyimide (low permittivity), FR-4 (high permittivity) substrates, and a partial ground plane of copper. The combined permittivity of both high and low permittivity substrate materials drastically reduces the overall permittivity, resulting in an antenna of a reasonable size that fits well in mobile devices. When just polyimide substrates are used, the size of the antenna gets too big to fit into mobile devices, and when only FR-4 substrates are used, the radiation efficiency suffers due to significant mismatch loss. Combining these substrates balances the degraded performance, radiation efficiency, and size issues of CSPA used in mobile device design. *Srivastava et. al.* [26]-[28] have designed the Cylindrical Surrounding Double-Gate (CSDG) MOSFET using various materials for the purpose of nanodevices.

Using dielectric constant of FR-4 ($\mathcal{E}_{r.fr\text{-}4}$) and polyimide ($\mathcal{E}_{r.pl}$) as *4.3* and *3.5*, the resultant dielectric constant ($\mathcal{E}_{R.r}$) and effective resultant dielectric constant ($\mathcal{E}_{R.eff.r}$) has been calculated as *3.9* and *3.15*, respectively. With the value of $\mathcal{E}_{R.r}$ and $\mathcal{E}_{R.eff.r}$, antenna dimensions like the width of ground (W_g), length of ground (L_g), the inner radius of groud (R_{gi}), the outer radius of ground (R_{go}), the outer radius of polyimide substrate ($R_{so.pl}$), the outer radius of FR-4 substrate ($R_{so.fr\text{-}4}$) and length of the substrate (Ls), Delta (ΔL), length of the patch (L_p), effective length (L_{eff}), inset feed length (Y_O), and width of feed (W_f) have been calculated and recorded in Table I. Also, the thickness of FR-4 ($H_{s.fr\text{-}4}$) and polyimide ($H_{s.pl}$) are *2.8* mm and *2.0* mm, respectively. (See Fig. 1)

TABLE I: DOUBLE MATERIAL CYLINDRICAL PATCH ANTENNA DESIGN PARAMETERS

Parameter	R_{g0}	R_{g1}	$R_{s0.pl}$	$R_{s0\text{-}fr\text{-}4}$	W_f	ΔL	L_p	W_g	L_s	L_g
Value (mm)	14.2	13.4	16.2	18	8.4	2.2	21.5	58.8	50.28	26.64

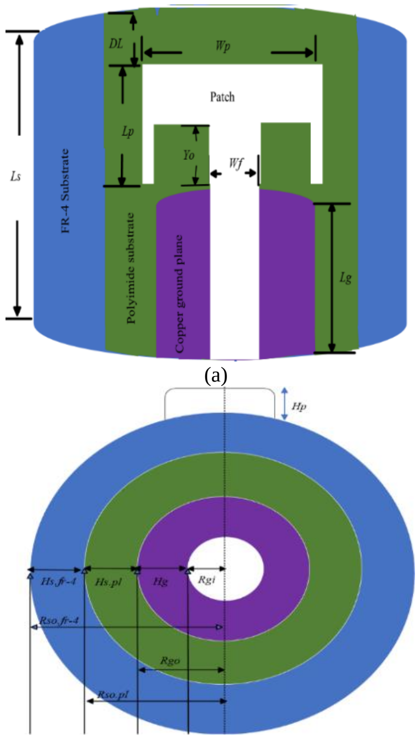

(a)

(b)

Fig. 1. Proposed DMS CSPA (a) front view and (b) bottom view [19].

III. Paramentric Analysis of Desigend Antenna

The quality factor may be described in three ways as a measure of antenna performance:

(i) Relationship between the antenna's stored reactive energy and its radiated power,

(ii) Measure of its admittance or impedance, and

(iii) Function of its bandwidth.

Each method has its physical meaning and results in various operating boundaries. Also, the surface current distribution of the antenna is observed to determine the antenna's radiation pattern at both resonance frequencies.

A. The Radiation Pattern of DMS CSPA

The far-field attributes are plotted as a function of spatial coordinates defined by elevation angle (Ɵ) and azimuth angle (ϕ). It's a graph showing radiated power per unit solid angle. It might be in the form of a polar, Cartesian, two-dimensional, or three-dimensional. Here the far-field plots have been presented in polar coordinates as presented in Fig. 2 to Fig. 5. The simulation experiment observed the E plane main lobe magnitude for *2.68* GHz and *5.55* GHz bands as *-51* dB and *-38.4* dB, signifying an increase in magnitude as resonance frequency increases as shown in Fig. 2.

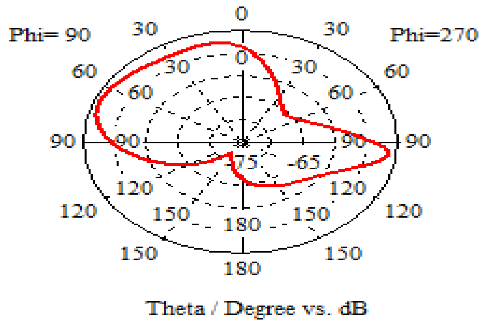

(a)

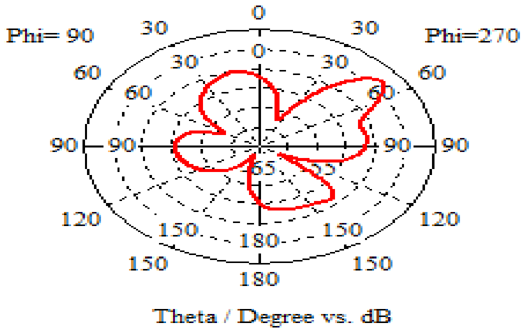

(b)

Fig. 2. Polar radiation pattern, showing main lobe magnitude E Plane: (a) 2.66 GHz, and (b) 5.55 GHz.

In Fig. 3, the angular width for the *2.68* GHz band decreases from *83.9* ^{0} to *45* ^{0} in the *5.55* GHz band, indicating a side lobe level of *-7.8 dB* and -4.1 dB for *2.68* GHz and *5.55* GHz band, respectively. Also, the main lobe direction for the *2.68* GHz and *5.55* GHz bands have been observed as *62* ^{0} and *113* ^{0}.

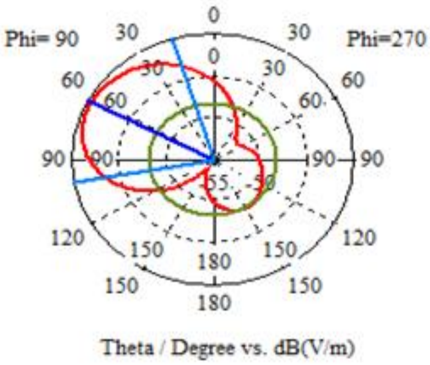

(a)

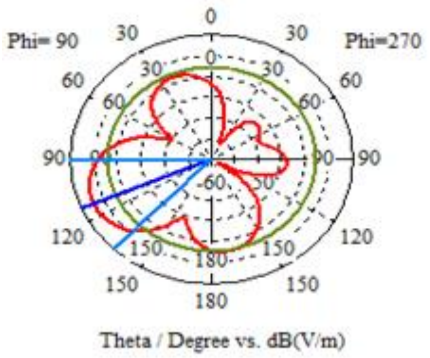

(b)

Fig. 3. Polar radiation pattern, showing sidelobe magnitude E Plane: (a) 2.66 GHz, and (b) 5.55 GHz.

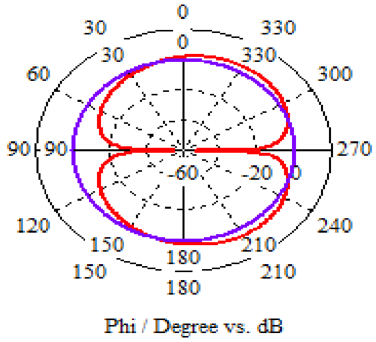

(a)

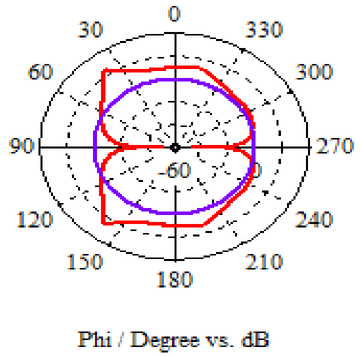

(b)

Fig. 4. Polar radiation pattern, showing main lobe magnitude H Plane: (a) 2.66 GHz, and (b) 5.55 GHz.

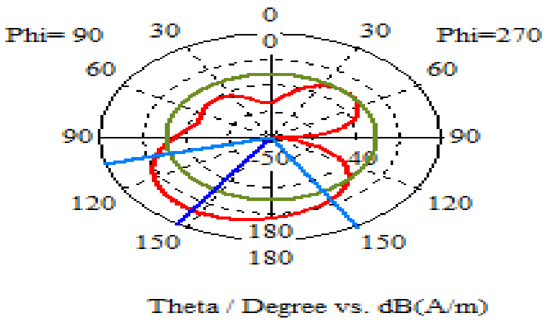

(a)

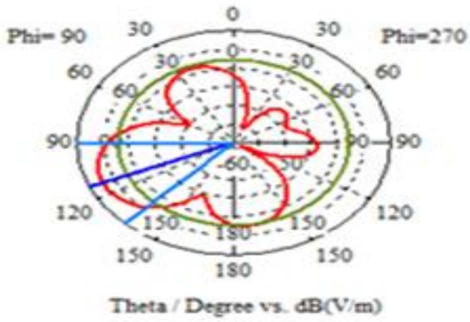

(b)

Fig. 5. Polar radiation pattern, showing sidelobe magnitude H-plane: (a) 2.66 GHz (b) 5.55 GHz.

Considering the polar radiation pattern presented in Fig. 4, the main lobe magnitude of *24* dB and *4.1* dB is observed, and values are within the acceptable main-lobe magnitude of regular CPAs. The H-plane side lobe angular width presented in Fig. 5 has been observed as *105*^{0} and

55.8^0, with main lobe directions of 146^0 and 132^0, respectively, for *2.66* GHz and *5.55* GHz bands. Also, the 2.68 GHz band presented the main lobe level of *-4.4* dB while the upper band (*5.55* GHz) is observed as *-11.9* dB.

In conclusion, the polar plots of the proposed DMS CSPA have shown a good and acceptable value of main-lobe magnitude, sidelobe level, angular width, angular width direction for E-planes and H-planes at both resonance frequencies.

However, main-lobe angular width values are greater than 45^0 at both resonance frequencies, indicating less directivity of the radiation patterns, making it suitable for application in mobile devices.

B. *Current Distribution*

The surface current distribution on the patch has been used to analyze the flow of current in the proposed microstrip patch antenna structure; current distributions have been simulated at the two resonant frequencies as demonstrated in Fig. 6.

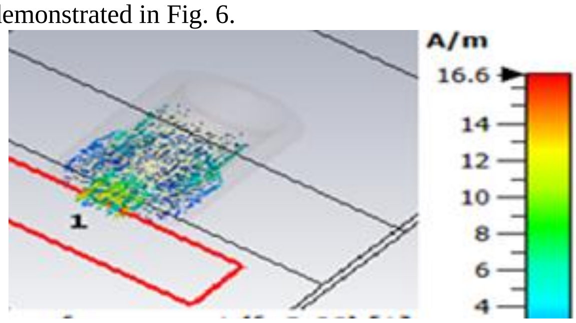

(a)

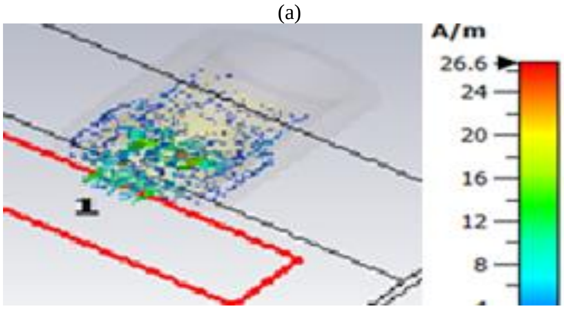

(b)

Fig. 6. Surface current distribution (a) 2.66 GHz (b) 5.55 GHz.

From the simulation experiment, the surface current distribution of the proposed DMS CSPA has been observed as *16.6315* A/m and *26.6302* A/m for the lower and upper band, respectively, as shown in Fig. 6.

The current is mostly concentrated in the radiator's corners at both frequencies. Furthermore, at *2.66* GHz, the surface current density is lower than the surface current density at *the 5.55* GHz band. Also, at *2.66* GHz, maximum current flows in the outer region of a patch, but at *5.55* GHz, current flows in the inner region. Again, at the input terminal of the DMS CSPA, the surface current density is more when compared with the opposite edge of a patch at both resonance frequencies.

C. *Total Quality Factor of Proposed DMS CSPA*

The advantage of using Q-factor as a parameter to measure the performance of conformal antennas is that it is dimensionless and values, either high or low, determine the bandwidth of any antenna design. Here, the total quality factor has been computed using equations in ref. [29], given as:

$$Q = \frac{F_C}{F_H - F_L} \tag{1}$$

where F_C, F_H, and F_L are center frequency, highest frequency, and lowest frequency of each band.

Since the proposed DMS CSPA has been observed to resonate at two frequency bands, *2.68* GHz (*2.28* GHz ~ *3.01* GHz) and *5.5 GHz* (*4.91* GHz ~ *6.1* GHz), the antenna Q for the *2.69 GHz* and *5.55* GHz band has been computed as *3.62* and *2.31*, respectively. Comparing the Q-factors at both resonance frequency, the *5.55* GHz band has been observed to have a smaller Q value indicating a larger bandwidth when compared with the *2.68* GHz band.

IV. Conclusions and Future Recommendations

In this research work, a DMS CSPA has been designed and simulated. The results were analyzed at resonant frequencies of *2.68* GHz and *5.55* GHz. Findings from the results show that though the DMS CSPA presented the good value of antenna Q and angular width of the main lobe at both resonance frequencies. The proposed antenna's less directivity and wider beamwidth make it suitable for usage in mobile devices requiring low directivity values.

This work can be extended by carrying out a physical implementation of the proposed model. Also, a MOSFET-based absorber and a circulator will be attached to the antenna to help solve the problem of impedance matching, should incase mismatch occur in the designed antenna.

Conflict of Interest

The authors declare no conflict of interest.

Author Contributions

Elliot O. Omoru (EOO) and Viranjay M. Srivastava (VMS) conducted this research; EOO designed and analyzed the model with data and wrote the paper; VMS has verified the result with the designed model; all authors had approved the final version.

References

[1] J. Kulkarni, R. Seenivasan, V. Abhaikumar, and D. R. P. Subburaj, "Design of a novel triple-band monopole antenna for WLAN/WiMAX MIMO applications in the laptop computer," *International Journal of Antennas and Propagation*, vol. 45, no. 6, pp. 257-267, Aug. 2019

[2] B. Hu, G. P. Gao, L. L. He, X. D. Cong, and J. N Zhao, "Bending and on-arm effects on a wearable antenna for 2.45 GHz body area network," *IEEE Antennas Wireless Propagation Letters*, vol. 15, pp. 378-81, June 2016

[3] M. Gustafsson and B. L. G. Jonsson, "Antenna Q and stored energy expressed in the fields, currents, and input impedance," *IEEE Transaction on Antennas and Propagation*, vol. 63, no. 1, pp. 240–249, 2015.

[4] Y. Zhang, H. Zheng, B. Gao, C. Tang, R. Liu, and M. Wang, "A compact dual-band antenna for 5G application," in *Proc. Cross Strait Quad-Regional Radio Science and Wireless Technology Conference*, China, July 2019, pp. 1-2.

[5] M. Agiwal, A. Roy, and N. Saxena, "Next generation 5G wireless networks: A comprehensive survey," *IEEE Communications Surveys & Tutorials*, vol. 18, no. 3, pp. 1617–1655, Feb. 2016.

[6] E. Amir, K. Veljko, G. Maria, and K. Gelareh, "Integration of 4G wireless technologies in a test-bed environment," *International Journal of Wireless & Mobile Networks*, vol. 5, no. 1, pp. 93-106, Feb. 2013

[7] B. Chen, Y. Jiao, F. Ren, and F. Zhang, "Dual wide-band open slot antenna with a band-rejected slit for 3.5/5.5GHz WiMAX and 5.2/5.8GHz WLAN applications," in *Proc. 4th IEEE International Symposium on Microwave, Antenna, Propagation and EMC Technologies for Wireless Communications*, China, Nov. 2011, pp. 113-115.

[8] A. A. Khan, M. H. Jamaluddin, S. A. J. Nasir, J. R. Kazim, and O. Owais, "Dual-band MIMO dielectric resonator antenna for WiMAX/WLAN applications," *IET Microwaves, Antennas & Propagation*, vol. 11, no. 1, pp. 113–120, Jan. 2017.

[9] D. Serghiou, M. Khalily, V. Singh, A. Araghi, and R. Tafazolli, "Sub-6 GHz dual-band 8 × 8 MIMO antenna for 5G smartphones," *IEEE Antennas and Wireless Propagation Letters*, vol. 19, no. 9, pp. 1546-1550, Sept. 2020.

[10] M. S. M. Mollaei, E. Zanganeh, and M. F. Farahani, "Enhancement of patch antenna gain using cylindrical shell-shaped superstrate," *IEEE Antennas and Wireless Propagation Letters*, vol. 16, pp. 2570-2573, Aug. 2017

[11] A. M. Mahros, M. M. Tharwat, and A. Elrashidi, "A novel performance analysis of the microstrip antenna printed on a cylindrical body," *International Journal of Antennas and Propagation*, vol. 2014, pp. 1-9, Dec. 2014.

[12] A. Elrashidi, K. Elleithy, and H. Bajwa, "The fringing field and resonance frequency of cylindrical microstrip printed antennaas a function of curvature," *International Journal of Wireless Communications and Networking*, vol. 3, no. 2, pp. 155–162, 2011.

[13] E. N. Umayah and V. M. Srivastava, "Comparative analysis of feeding techniques for cylindrical surrounding patch antenna," *International Journal of Electrical and Computer Engineering*, vol. 10, no. 5, pp. 5377-5384, Oct. 2020.

[14] Y. Liu, L. M. Si, M. Wei, P. Yan, P. Yang, H. Lu, C. Zheng, Y. Yuan, J. Mou, L. Xin, and H. Sun, "Some recent developments of microstrip antenna," *International Journal of Antennas and Propagation*, vol. 2012, pp. 1-10, March 2012.

[15] X. S. Fang and K. W. Leung "Linear-/circular-polarization designs of dual-/wide-band cylindrical dielectric resonator antennas," *IEEE Transactions on Antennas and Propagation*, vol. 60, no. 6, pp. 2662–2671, April 2012.

[16] D. Guha, A. Banerjee, C. Kumar, and Y. M. M. Antar, "Higher order mode excitation for high-gain broadside radiation from cylindrical dielectric resonator antennas," *IEEE Transactions on Antennas and Propagation*, vol. 60, no. 1, pp. 71-77, Jan. 2012.

[17] T. Liu, H. Yang, Y. He, and J. Lu, "Cylindrical ring dielectric loaded horizontally polarized omnidirectional antenna for wide-band radiation," *AEU - International Journal of Electronics and Communications*, vol. 90, pp. 123-129, April 2018.

[18] M. C. Scardelletti, N. Dib, T. Weller, J. Culver, and B. King, "Cylindrical ring dielectric loaded horizontally polarized omnidirectional antenna for wide-band radiation," *AEU - International Journal of Electronics and Communications*, vol. 59, pp. 25-30, Jan. 2005.

[19] E. O. Omoru and V. M. Srivastava, "Bandwidth and return loss improvement technique using double material substrate cylindrical surrounding patch antenna: Part I," *International Journal of Engineering Trends and Technology*, vol. 69, no. 12, Dec. 2021.

[20] C. L. Wen and Q. X. Chu, "A Bandwidth enhanced broadband patch antenna for LTE700/GSM850/GSM900 applications," in *Proc*. *Cross Strait Radio Science & Wireless Technology Conference* (CSRSWT), China, Dec. 2020, pp. 1-3.

[21] T. Mikulasek, A. Georgiadis, A. Collado, and J. Lacik, "2× 2 Microstrip patch antenna array fed by substrate integrated waveguide for radar applications," *IEEE Antennas and Wireless Propagtion Letters*, vol. 12, pp. 128-1290, Sep. 2013.

[22] A. A. Rimon, A. Samaddar, and N. I. Shawn, "A wide-band microstrip patch antenna using FR4 substrate," *International Journal of Advanced Research in Electrical, Electronics and Instrumentation Engineering*, vol. 4, no. 7, pp. 6667-6671, July 2015.

[23] L. C. Paul, M. S. Hosain, and S. Sarker, "The effect of changing substrate material and thickness on the performance of inset feed microstrip patch antenna," *American Journal of Networks and Communications*, vol. 4, no. 3, pp. 54-58, May 2015.

[24] G. Singh, R. Rajni, and R. S. Momi, "Microstrip patch antenna with defected ground structure for bandwidth enhancement," *International Journal of Computer Applications*, vol. 73, no. 9, pp. 14-18, July 2013.

[25] E. O. Omoru and V. M. Srivastava, "MOSFET based absorber for reflected signal in 5G massive MIMO base station - A circuit perspective," *Journal of Communications*, vol. 15, no. 11, pp. 833-840, Nov. 2020.

[26] V. M. Srivastava, K. S. Yadav, and G. Singh, "Design and performance analysis of cylindrical surrounding double-gate MOSFET for RF switch," *Microelectronics Journal*, vol. 42, no. 10, pp. 1124-1135, Oct. 2011

[27] U. A. Maduagwu and V. M. Srivastava, "Sensitivity of lightly and heavily dopped cylindrical surrounding double-gate (CSDG) MOSFET to process variation," *IEEE Access*, vol. 9, pp. 142541-142550, Oct. 2021.

[28] N. Gowthaman and V. M. Srivastava, "Capacitive modeling of CSDG MOSFETs for hybrid RF applications," *IEEE Access*, vol. 9, pp. 89234-89242, June 2021.
[29] C. A. Balanis, *Antenna theory Analysis and Design,* 4th Ed., John Wiley & Sons, Inc., Hoboken, New Jersey, USA, 2016.

Er. Elliot O. Omoru received Bachelor of Engineering degree in Computer Engineering from University of Benin, Master of Science in Electronics Engineering from University of KwaZulu-Natal, Durban South Africa. Presently, he is working towards doctoral research with the department of Electronic Engineering, University of KwaZulu-Natal, Durban South Africa. He has published various peer-reviewed articles in Journals and Conferences. His major research area is microwave and millimeter wave engineering, filter design, antenna design and analogue electronics.

Prof. Viranjay M. Srivastava is a Doctorate (2012) in the field of RF Microelectronics and VLSI Design, Master (2008) in VLSI design, and Bachelor (2002) in Electronics and Instrumentation Engineering. He has worked on the fabrication of devices and development of circuit design. Presently, he is working in the Department of Electronic Engineering, Howard College, University of KwaZulu-Natal, Durban, South Africa. He has more than 19 years of teaching and research experience in the area of VLSI design, RFIC design, Antenna design, and Analog IC design. He has supervised various Bachelors, Masters and Doctorate theses.
Prof. Srivastava is a Professional Engineer of ECSA, South Africa and Life member of IEEE-HKN, Senior members of IEEE, SAIEE, and members of IET, IITPSA. He has worked as a reviewer for several Journals and Conferences, both national and international. He is author/co-author of more than 290 scientific contributions, including articles in international refereed Journals and Conferences and also the author of various books.